New Journal of Physics
An Institute of Physics and Deutsche Physikalische Gesellschaft Journal

Photodetachment cross sections of the positronium negative ion

Akinori Igarashi[1], **Isao Shimamura**[2] **and Nobuyuki Toshima**[3]

[1] Faculty of Engineering, Miyazaki University, Miyazaki 889-2192, Japan
[2] RIKEN (Institute of Physical and Chemical Research), Wako, Saitama 351-0198, Japan
[3] Institute of Materials Science, University of Tsukuba, Tsukuba 305-8573, Japan

New Journal of Physics **2** (2000) 17.1–17.14 (http://www.njp.org/)
Received 10 May 2000; online 23 August 2000

Abstract. The cross sections for the photodetachment from a weakly bound positronium negative ion Ps^- below the threshold for the formation of $Ps(n = 4)$ are calculated using the hyperspherical close-coupling method, and are compared with the corresponding spectra for the H^- ion. Detailed resonance structures in the spectra near the $Ps(n = 2, 3$ and $4)$ thresholds are reported for the first time. The off-resonance cross section below the $Ps(n = 2)$ threshold differs appreciably from that obtained by a variational calculation (Ward *et al* 1987 *J. Phys. B: At. Mol. Phys.* **20** 127), but agrees well with the recent close-coupling calculations with a B-spline expansion (Igarashi *et al* 2000 *Phys. Rev.* A **61** 032 710). The resonance energies and widths of the $^1P^o$ symmetry are generally in good agreement with the results of the complex-coordinate rotation calculation.

1. Introduction

The positronium negative ion, $Ps^-(e^+e^-e^-)$, is one of the systems in which three particles with equal mass interact through Coulomb potentials. As other much weaker interactions are neglected, similar systems such as $\mu^+\mu^-\mu^-$ and $\bar{p}pp$ should show, essentially, the same physics as Ps^- because the non-relativistic Hamiltonian of these systems exactly scales with mass. In other words, the Schrödinger equation for these systems takes exactly the same form if the energy and length scaled with the mass are used. The Ps^- ion has only one bound state of symmetry $^1S^e$ with an extremely small binding energy ϵ_0 of 0.012 005 07 a.u. (atomic units) [1]. Its existence was experimentally confirmed [2] and the decay rate was measured to be $2.09 \pm 0.09\ ns^{-1}$ [3], which is in good agreement with theoretical predictions.

1367-2630/00/000017+14$30.00

The Ps^- ion is also one extreme example of two electrons bound simultaneously to a particle with a unit positive charge. The other extreme is the negative hydrogen ion H^- (and its isotopes D^- and T^-). It would be of great interest to elucidate the change in the dynamics of the bound, continuum and resonance states of these systems as the mass of the positively charged particle decreases from the proton down to the positron.

Whereas no experimental measurement has been carried out for Ps^- photodetachment or $e^- + Ps$ scattering, Ps beams have recently become available and direct measurements of the total cross sections of the Ps scattering by simple atomic and molecular systems have been reported [4]. Thus, the experimental studies of the continuum states of the Ps^- system may be plausible in the near future.

Theoretically, some studies have been made on the dynamics of the Ps^- system. In particular, Ward *et al* [5] calculated variationally the $e^- + Ps$ elastic and Ps^- photodetachment cross sections below the threshold for $Ps(n = 2)$, although the cross sections in the resonance region below this threshold were not shown in detail. Bhatia and Drachman [6] and Ermolaev and Mandal [7] obtained the cross sections of $Ps(n = 1)$ production by photodetachment of Ps^- by model calculations that are valid only in a narrow energy region near the detachment threshold. Botero and Greene [8] made a semi-quantitative estimation of the resonances (of $^1P^o$ symmetry) in the photodetachment cross sections near the $Ps(n = 2)$ threshold by an adiabatic treatment in the hyperspherical-coordinate representation. Resonances of $^1P^o$ symmetry were also studied using the complex-coordinate rotation method with Hylleraas-type basis functions [9]–[12]. This method was extended for other symmetries; see [12] and references therein. Recently, Igarashi *et al* [13] used a close-coupling method with a B-spline expansion and calculated the off-resonance Ps^- photodetachment cross section below the $Ps(n = 2)$ threshold.

It is now generally recognized that the hyperspherical coordinate system is much more appropriate for the study of the dynamics of strongly correlated three-body systems than the conventional independent-particle coordinate system. The pioneering work by Macek [14] and subsequent studies of two-electron atoms [15, 16] clearly indicated the usefulness of adiabatic hyperspherical potentials, or the potential energy curves drawn as functions of the hyper-radius $\rho = \sqrt{r_1^2 + r_2^2}$ (with the radial coordinates r_1 and r_2 of the two electrons), in understanding the physics of the bound and resonance states both visually and numerically in analogy with adiabatic molecular potential curves. A great improvement in the numerical accuracy was achieved by taking the non-adiabatic coupling into account; the close-coupling method in terms of hyperspherical coordinates, or the hyperspherical close-coupling (HSCC) method, was found to be a powerful tool for studying strong electron–electron correlation effects in two-electron systems such as He and H^- [15, 16]. It has been successfully applied to the calculations of photoionization and photodetachment cross sections; see, for example, [17, 18]. It would be interesting to see the applicability of the HSCC method to the Ps^- system, and to compare the photodetachment cross sections between Ps^- and H^-. In fact, we applied the HSCC method to S- and P-wave elastic scattering and the *ortho*-to-*para* Ps conversion process in electron collisions with Ps in a previous publication [19]. S-wave scattering of electrons by Ps was also treated by Zhou and Lin [20] by the use of the HSCC method.

In this work, we calculate the cross sections $\sigma(\hbar\omega; n)$ for photodetachment

$$\hbar\omega + Ps^- \rightarrow e^- + Ps(n) \tag{1}$$

for photon energies below the Ps($n = 4$) production threshold, and obtain resonance parameters of the $^1\mathrm{P^o}$ symmetry from the continuum calculations. Atomic units are used throughout this paper unless otherwise stated.

2. The HSCC method

We first define two sets of Jacobi coordinates ($\boldsymbol{r}_i$, $\boldsymbol{R}_i$) ($i = 1, 2$), where $\boldsymbol{r}_i$ is the position vector of the ith electron e_i measured from the positron, and where $\boldsymbol{R}_i$ is the relative-distance vector from the centre of mass of the electron–positron pair to the other electron. The hyper-radius ρ is defined by

$$\rho^2 = \tfrac{2}{3}R_i^2 + \tfrac{1}{2}r_i^2 \tag{2}$$

which turns out to be the same for $i = 1$ and for $i = 2$. Here, the coefficient of a half is the reduced mass of Ps and the coefficient of two-thirds is the reduced mass between Ps and the remaining electron. In the following, the internal motion of Ps^- is described, not in terms of the Jacobi coordinates, but in terms of ρ and five angular coordinates ($\hat{\boldsymbol{r}}_i$, $\hat{\boldsymbol{R}}_i$, $\phi_i \equiv \tan^{-1}\{(\sqrt{3}/2)r_i/R_i\}$), denoted collectively by Ω. The total Hamiltonian H of the system Ps^- is divided into a part stemming from the kinetic-energy operator in ρ and the rest, h_{ad}, which is adiabatic in ρ. Thus we have

$$H = -\frac{1}{2}\left(\frac{\mathrm{d}}{\mathrm{d}\rho^2} + \frac{5}{\rho}\frac{\mathrm{d}}{\mathrm{d}\rho}\right) + h_{ad}(\rho;\Omega) \tag{3}$$

with

$$h_{ad} = \frac{\boldsymbol{\Lambda}^2}{2\rho^2} + V(\rho,\Omega) \tag{4}$$

where $V(\rho,\Omega)$ is the sum of all the Coulomb interactions in Ps^-. The operator $\boldsymbol{\Lambda}$ is the five-dimensional grand angular momentum in Ω [14], whose square may be written as

$$\boldsymbol{\Lambda}^2 = -\frac{1}{\sin^2\phi_i\cos^2\phi_i}\left(\frac{\mathrm{d}}{\mathrm{d}\phi_i}\sin^2\phi_i\cos^2\phi_i\frac{\mathrm{d}}{\mathrm{d}\phi_i}\right) + \frac{\boldsymbol{L}_{R_i}^2}{\cos^2\phi_i} + \frac{\boldsymbol{L}_{r_i}^2}{\sin^2\phi_i} \qquad (i = 1, 2) \tag{5}$$

in terms of the angular-momentum operators $\boldsymbol{L}_{R_i}$ and $\boldsymbol{L}_{r_i}$ conjugate to the angles $\hat{\boldsymbol{R}}_i$ and $\hat{\boldsymbol{r}}_i$.

The adiabatic channel functions $\{\varphi_\mu\}$ and the adiabatic potentials $\{U_\mu(\rho)\}$ are the eigenfunctions and the eigenvalues of the adiabatic Hamiltonian h_{ad}, which contains ρ as the adiabatic parameter:

$$h_{ad}(\rho;\Omega)\varphi_\mu(\rho;\Omega) = \left(U_\mu(\rho) - \frac{15}{8\rho^2}\right)\varphi_\mu(\rho;\Omega). \tag{6}$$

As $\rho \to \infty$, φ_μ describes a fragmentation limit $\mathrm{e}^- + \mathrm{Ps}$ and U_μ approaches the energy of this Ps.

In the HSCC method the total wavefunction $\Psi(\rho,\Omega)$ is expanded in the form

$$\Psi(\rho,\Omega) = \sum_\mu \rho^{-5/2}F_\mu(\rho)\varphi_\mu(\rho;\Omega). \tag{7}$$

Substitution of this expansion into the Schrödinger equation of the total system leads to coupled radial equations

$$\left(-\frac{1}{2}\frac{\mathrm{d}^2}{\mathrm{d}\rho^2} + U_\mu(\rho) - E\right)F_\mu(\rho) + \sum_\nu V_{\mu\nu}F_\nu(\rho) = 0 \tag{8}$$

where $V_{\mu\nu}$ represents the non-adiabatic coupling following from the differential operators on the right-hand side of (3) [21]. The procedure for solving the radial coupled equations is essentially the same as for the muon-transfer problem treated in [21].

The solutions in the hyperspherical coordinates are matched with the asymptotic solutions in the Jacobi coordinates at some point $\rho = \rho_M$. For these asymptotic solutions for $\rho \geq \rho_M$, we use a dipole representation [22] in which the continuum electron is described as a particle moving in the dipole field of the excited Ps atom, just as was done in [18].

The adiabatic channel functions φ_μ in (6) are calculated by a variational method using a trial function for the ^{2S+1}L symmetry with basis functions

$$(\cos\phi_1)^{l_2} r_1{}^{l_1+n} \mathrm{e}^{-\alpha r_1} \mathcal{Y}^L_{l_1 l_2}(\hat{\boldsymbol{r}}_1, \hat{\boldsymbol{R}}_1) + (-1)^S (\cos\phi_2)^{l_2} r_2{}^{l_1+n} \mathrm{e}^{-\alpha r_2} \mathcal{Y}^L_{l_1 l_2}(\hat{\boldsymbol{r}}_2, \hat{\boldsymbol{R}}_2). \tag{9}$$

The angular function $\mathcal{Y}^L_{l_1 l_2}(\hat{\boldsymbol{r}}_i, \hat{\boldsymbol{R}}_i)$ is a simultaneous eigenfunction of $\boldsymbol{L}^2_{r_i}$, $\boldsymbol{L}^2_{R_i}$, and $(\boldsymbol{L}_{r_i} + \boldsymbol{L}_{R_i})^2$ with eigenvalues $l_1(l_1+1)$, $l_2(l_2+1)$, and $L(L+1)$, respectively. In the present calculation, 18 s, 16 p, 14 d, and 12 f orbitals (with $l_1 = 0$, 1, 2, and 3) are used, with all possible l_2 values that couple with these l_1 and produce the right value of L.

The photodetachment cross section $\sigma(\hbar\omega; n)$ is calculated from the dipole matrix element $\langle \Psi_f(n) | D | \Psi_i \rangle$. Here, D is the dipole operator in the length or velocity form, Ψ_i the initial bound state of the $^1\mathrm{S^e}$ symmetry, and Ψ_f the final continuum state of the $^1\mathrm{P^o}$ symmetry with the boundary condition appropriate for the production of Ps(n) in the electron emission. The HSCC method is used consistently for calculating both the bound and the continuum wavefunctions.

3. Results and discussion

The wavefunctions for the initial and the final states are calculated using all the channel functions associated with $\mathrm{e}^- + \mathrm{Ps}(n = 1\text{–}4)$ in the asymptotic region. The obtained energy of the initial bound state is $-0.261\,999$ compared well with the recent, highly accurate theoretical value of $-0.262\,005$ [1].

The matching radius ρ_M for the calculation of the continuum wavefunction is chosen as 720, since the photodetachment cross sections calculated with $\rho_M = 720$ and with $\rho_M = 920$ differed by less than 1% even near thresholds and since they turned out to be stable against the change in ρ_M for $\rho_M \geq 720$. The dipole matrix element is calculated by a radial integration over the range $0 \leq \rho \leq 325$.

The photodetachment cross sections obtained in the length and the velocity forms of the dipole operator should be exactly the same if the wavefunctions used in the dipole–matrix calculations were exact, although the gauge independence (or the same results from the length and velocity forms) does not always guarantee the exact wavefunctions. The present results with both gauges agree within 1% and, hence, here we report only the results from the length form. The appendix explains how we assess the convergence of the photodetachment cross section $\sigma(\hbar\omega; n)$ for the production of Ps(n), with respect to the number of channels included in the HSCC equations for the final continuum state. As is explained in the appendix, the inclusion of all channels up to $\mathrm{e}^- + \mathrm{Ps}(n = 4)$ is expected to lead to quite accurate cross sections except very close to the threshold $E_{\mathrm{Ps}(n=4)} = -0.015\,625$ for the formation of Ps($n = 4$).

The calculated total photodetachment cross section $\sum_n \sigma(\hbar\omega; n)$ is shown in figure 1 below a photon energy of 6.7 eV in comparison with three other calculations. One is an estimation by Bhatia and Drachman [6] using the asymptotic wavefunction

$$\Psi_i = C[R_i^{-1} \exp(-\gamma R_i)] \psi_{\mathrm{Ps(1s)}}(\boldsymbol{r}_i) \tag{10}$$

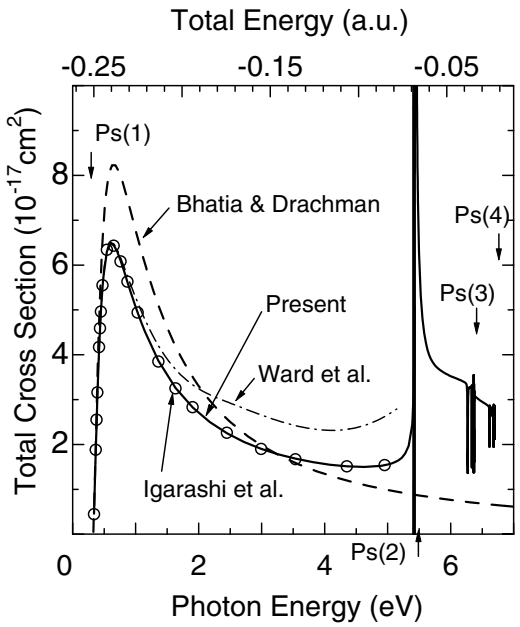

Figure 1. The total cross section for photodetachment $\hbar\omega + \mathrm{Ps}^- \rightarrow \mathrm{e}^- + \mathrm{Ps}$ below the Ps($n = 4$) threshold. Full curve, present calculation; dashed curve, Bhatia and Drachman [6]; dot–dashed curve, Ward *et al* [5]; and open circles, Igarashi *et al* [13]. The threshold energies for the production of Ps(n) are indicated by vertical arrows.

for the initial bound state and the properly symmetrized product of the Ps ground-state wavefunction $\psi_{\mathrm{Ps(1s)}}(\boldsymbol{r}_i)$ and a plane wave of the relative coordinate $\boldsymbol{R}_i$ for the final state. In equation (10), γ satisfies $\epsilon_0 = (3/4)\gamma^2$, and the normalization constant C is determined to reproduce well the asymptotic form of an accurate Ps^- wavefunction. This simple approximation for the photodetachment cross section is a modification of the method applied to the photodetachment of H^- by Ohmura and Ohmura [23]. This approximation is valid only for low photoelectron energies for which the p-wave photoelectron is kept away from the inner region by the centrifugal barrier and has a small phase shift, and for which the main contribution to the dipole matrix element comes from a region where the photoelectron lies far from the neutral H or Ps atom.

Another, more elaborate calculation included in figure 1 was carried out by Ward *et al* [5] by means of the variational method below the Ps($n = 2$) threshold. The cross section of Ward *et al* agrees well with the present results below 0.6 eV, where the cross section reaches its maximum. At higher photon energies, however, a considerable difference is found between them. The cross section of Ward *et al* is about 50% larger than the present HSCC results near 4 eV. For confirming the reliability of the present results we carried out a detailed convergence test not only as described in the appendix, but also by reducing the number of coupled equations for both the initial and final states to only the Ps($n = 1, 2$) channels. All of these test calculations yielded nearly the same photodetachment cross sections around 5 eV and below, showing the good convergence of the present cross section, although the reduced coupled equations deteriorated the initial-state binding energy ϵ_0 to 0.011 974, compared with the value 0.011 999 obtained in the full calculation. As a further check of the numerical calculations we obtained the photodetachment

Table 1. The phase shifts for scattering $e^- + Ps(n = 1)$ of $^1P^o$ symmetry at energies below the $Ps(n = 2)$ threshold. The total energy of the system is given by $E = \frac{3}{4}k^2 - 0.25$ in atomic units in terms of the wavenumber k of the relative motion. The present results are shown for two different sizes of the HSCC equations, namely, including all channels detaching into $e^- + Ps(n = 1, 2)$ and including all channels $e^- + Ps(n = 1–4)$. Comparison is made with the variational calculation by Ward *et al* [5] and with the B-spline close-coupling calculation by Igarashi *et al* [13].

k	E	$Ps(n = 1, 2)$	$Ps(n = 1–4)$	Ward *et al*	Igarashi *et al*
0.05	−0.2481	−0.0044	−0.00026	−0.0006	—
0.10	−0.2425	−0.0485	−0.0425	−0.038	−0.0379
0.15	−0.2331	−0.140	−0.0130	−0.123	—
0.20	−0.2200	−0.258	−0.244	−0.235	−0.235
0.25	−0.2031	−0.383	−0.365	−0.353	—
0.30	−0.1825	−0.501	−0.477	−0.463	−0.463
0.35	−0.1581	−0.604	−0.575	−0.559	—
0.40	−0.1300	−0.688	−0.654	−0.635	−0.634
0.45	−0.0981	−0.748	−0.708	−0.687	—

cross sections of H^- by replacing the positron mass with the proton mass, and found a satisfactory agreement with the cross sections found in the literature [18, 24, 25].

The third calculation compared in figure 1 with the present results is an elaborate close-coupling calculation with B-spline expansion by Igarashi *et al* [13]. The agreement is seen to be perfect.

Table 1 compares the phase shifts for scattering $e^- + Ps(n = 1)$ of $^1P^o$ symmetry calculated using two different sets of HSCC equations with those obtained by Ward *et al* [5] and by Igarashi *et al* [13]. The present values for the larger set of coupled equations are close to the results of Ward *et al* and Igarashi *et al*; the difference in the phase shifts is too small to explain the large difference, found in figure 1, in the photodetachment cross sections between the present calculation and that of Ward *et al*. Calculated photodetachment cross sections are usually more stable than the phase shifts with respect to an increase in the number of coupled channels, since the former are obtained from the dipole matrix element between the initial and the final wavefunctions, which is insensitive to the small change in the phase of the wavefunction. Thus, the reason for the disagreement between the present cross section and that of Ward *et al* is unclear.

One of the oscillator-strength sum rules [26]

$$S_{-1} \equiv (2\pi^2\alpha)^{-1} \int_{\epsilon_0}^{\infty} \mathrm{d}(\hbar\omega) \sum_n \sigma(\hbar\omega; n)/(\hbar\omega)$$
$$= \frac{8}{27}\langle\Psi_i|(\boldsymbol{r}_1 + \boldsymbol{r}_2)^2|\Psi_i\rangle \equiv \tilde{S} \tag{11}$$

where α is the fine-structure constant, was used by Bhatia and Drachman [6] for a consistency check. This check was made also by Ward *et al* [5]. They reported a close agreement, namely, $S_{-1} = 29.5$ and $\tilde{S} = 29.75$. In this check, however, they used the cross section above the $Ps(n = 2)$ threshold calculated in the asymptotic approximation of [6], since they carried out the variational calculation only below this threshold. As mentioned below equation (10), the

asymptotic approximation is valid only for low photon energies near the detachment threshold. Indeed, the cross section in the asymptotic approximation differs significantly from that of other, more accurate calculations shown in figure 1 even at a low energy of 0.6 eV. Furthermore, the contribution from the Ps production in excited states and the resonance effect on the photodetachment cross sections are also important for an accurate evaluation of S_{-1}; neither of them is taken into account in the asymptotic approximation. Therefore, the apparent agreement between S_{-1} and $\tilde{S}$ of Ward *et al* does not necessarily suggest the accuracy of their cross sections.

In the present calculation, $\tilde{S}$ is found to be 29.79 and the contribution to S_{-1} from the region below the Ps($n = 2$) threshold $E_{\mathrm{Ps}(n=2)}$ is 25.16. The latter value is to be compared with the corresponding contribution 28.0 in the length form in the calculation by Ward *et al* †. The larger value of Ward *et al* is naturally expected from figure 1.

The present contribution to S_{-1} from the region between the Ps($n = 2$) and Ps($n = 3$) thresholds is 1.80 and that from the region between the Ps($n = 3$) and Ps($n = 4$) thresholds is 0.36, all the contributions up to the Ps($n = 4$) threshold summing up to 27.32, which is still less than 29.79 by 2.47 ($\equiv \Delta S_{-1}$). The oscillator-strength sum S_0 up to the Ps($n = 4$) threshold is 1.917 (1.389 from $E < E_{\mathrm{Ps}(n=2)}$, 0.431 from $E_{\mathrm{Ps}(n=2)} < E < E_{\mathrm{Ps}(n=3)}$, and 0.097 from $E_{\mathrm{Ps}(n=3)} < E < E_{\mathrm{Ps}(n=4)}$), and is still less than the correct value of 2.000 by 0.083. This missing contribution, which should come from the region above the Ps($n = 4$) threshold, is expected to explain a large part of the difference ΔS_{-1}.

In figure 1 for the total photodetachment cross section, we see sharp spikes in the neighbourhood of the Ps($n = 2$) threshold (at 5.4287 eV in photon energy) and structures below the $n = 3$ (6.3736 eV) and $n = 4$ (6.7043 eV) thresholds. An energy region near the Ps($n = 2$) threshold is enlarged in figure 2 for the partial cross sections $\sigma(\hbar\omega; n)$ ($n = 1, 2$) where a comparison is made with the cross section for photodetachment from H^-. Two prominent spikes just below the Ps($n = 2$) or H($n = 2$) threshold are due to the first two of the infinite series of Feshbach resonances. These resonances are attributed to energy levels supported by an attractive adiabatic hyperspherical potential that decays as ρ^{-2} owing to the Stark effect on the degenerate Ps($n = 2$) or H($n = 2$) states. Another peak above the Ps($n = 2$) or H($n = 2$) threshold arises from a shape resonance of $^1\mathrm{P^o}$ symmetry. These resonances are discussed, for example, in [8].

The channel functions in (6) contain the information on the correlation patterns between the particles and they are reflected in the shape of the corresponding adiabatic potential curves. After [27], we use the label $n(K,T)^A$ to specify a channel or a potential curve and use a set of quantum numbers $n(K,T)^A_{n'}$ to assign a resonance which is mainly supported by the $n(K,T)^A$ potential curve and for which the inner (outer) electron is interpreted to be in the orbital with a radial quantum number n (n')‡. A channel function with n describes the fragmentation into $e^- + \mathrm{Ps}(n)$ in the asymptotic region, and its potential curve approaches the energy of Ps(n). The quantum number K is related to the average of the vectorial distance $\boldsymbol{r}_i$ between the two particles in Ps(n) projected onto the relative vector $\boldsymbol{R}_i$ between Ps and the other electron. The quantum number T is related to the average of the total angular momentum projected onto the interelectronic axis. A channel function with $A = +\,(-)$ has an antinodal (nodal) structure near $r_1 = r_2$, while that with $A = 0$ has much less amplitude there; A represents the radial correlation

† This value was estimated by subtracting from the value of S_{-1} quoted in [5] the contribution from the region above the Ps($n = 2$) threshold calculated in the asymptotic approximation.

‡ The radial quantum number n' for the outer electron is assumed to start from n and to increase one by one in a particular series, although its meaning deviates from the Rydberg principal quantum number.

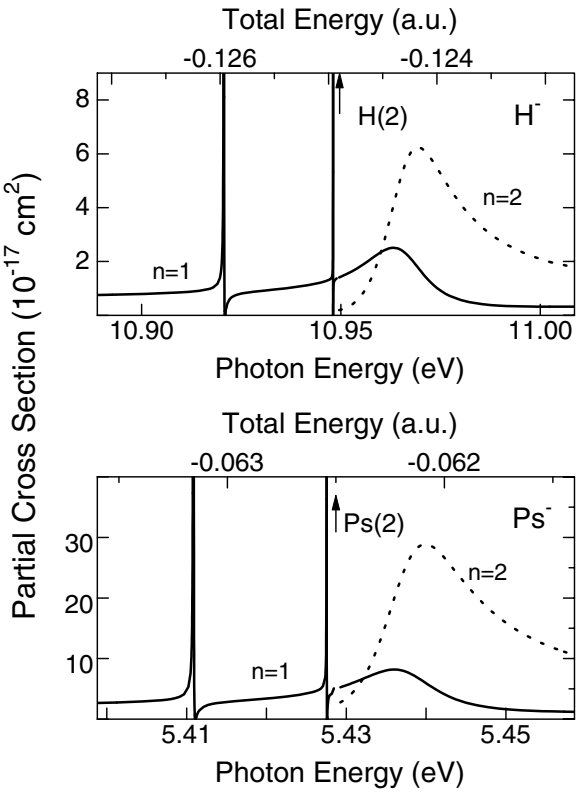

Figure 2. Partial photodetachment cross sections for $\hbar\omega + \mathrm{H}^- \rightarrow \mathrm{e}^- + \mathrm{H}(n)$ and $\hbar\omega + \mathrm{Ps}^- \rightarrow \mathrm{e}^- + \mathrm{Ps}(n)$ near the $n = 2$ threshold indicated by vertical arrows. Full curve, $n = 1$ production; and dotted curve, $n = 2$ production.

or the correlation between r_1 and r_2. The rules specified in [27] for the case of He and H^- have been applied to assign the $(K, T)^A$ quantum numbers to each of the Ps^- potentials. Channels with larger K in each manifold have lower-lying potentials as $\rho \rightarrow \infty$ than those with smaller K. For small ρ, $A = +$ channels are more attractive than $A = -$ channels.

The $^1\mathrm{P^o}$ potential curves converging to the $n = 3$ ($n = 4$) thresholds in the asymptotic region are shown in figure 3 (figure 4). The potentials $3(1, 1)^+$ and $3(2, 0)^-$ in figure 3 and $4(3, 0)^-$, $4(2, 1)^+$, and $4(1, 0)^-$ in figure 4 are attractive in nature at large ρ, due to the dipole potentials resulting from the degenerate excited states Ps($n = 3$) or Ps($n = 4$). They support infinite series of Feshbach resonances. The law of a constant energy ratio between adjacent resonances in a particular series, derived by Gailitis and Damburg [22], may be used to identify the series.

The partial photodetachment cross sections $\sigma(\hbar\omega; n)$ below the $n = 3$ ($n = 4$) threshold are shown in figure 5 (figure 6) for the H^- and Ps^- systems. We see that the resonances supported by the channels with $A = +$ have broader widths than the $A = -$ resonances. The main decay channels satisfy $\Delta n = -1$ and $\Delta K = -1$ with T and A unchanged [28], namely, $3(1, 1)^+ \rightarrow 2(0, 1)^+$ and $4(2, 1)^+ \rightarrow 3(1, 1)^+$ for the $A = +$ channels and $3(2, 0)^- \rightarrow 2(1, 0)^-$ and $4(3, 0)^- \rightarrow 3(2, 0)^-$ for the $A = -$ channels. A channel with $A = +$ has a deeper minimum at a smaller ρ than a channel with $A = -$. This leads to a larger overlap and stronger non-adiabatic coupling between $n(K, T)^A$ and $(n - 1)(K - 1, T)^A$ for $A = +$ than for $A = -$ and, hence, to broader $A = +$ resonances than $A = -$ resonances.

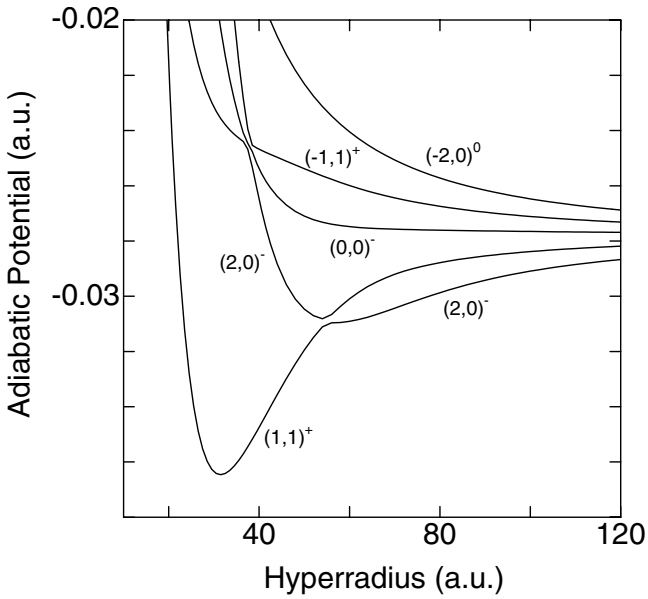

Figure 3. The $^1\mathrm{P^o}$ potential curves converging to the Ps($n = 3$) threshold in the asymptotic region. A set of quantum numbers $(K, T)^A$ is attached to each curve.

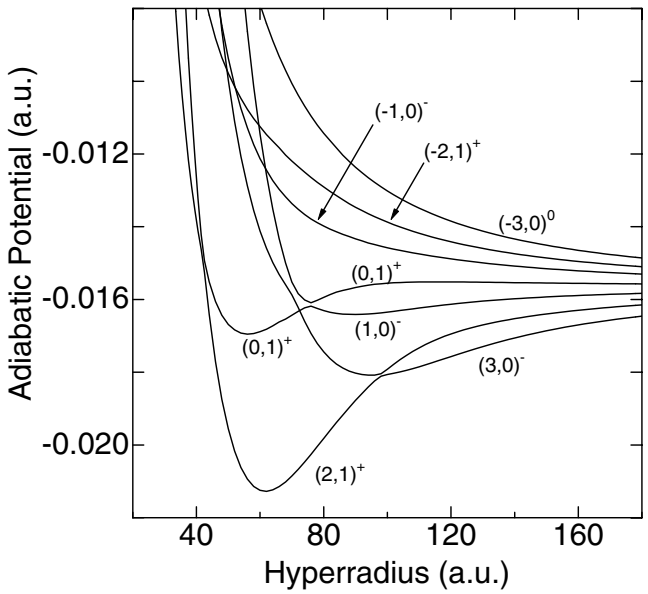

Figure 4. The $^1\mathrm{P^o}$ potential curves converging to the Ps($n = 4$) threshold in the asymptotic region. A set of quantum numbers $(K, T)^A$ is attached to each curve.

A close qualitative resemblance between the photodetachment spectra of $\mathrm{Ps^-}$ and $\mathrm{H^-}$ is seen in figure 2 up to the energy region of the shape resonance near the Ps($n = 2$) threshold. For energies near and above the $3(1, 1)_3^+$ resonance in figure 5, there still exist corresponding resonances in $\mathrm{Ps^-}$ and $\mathrm{H^-}$, but the detailed shape begins to differ depending on the system. The $4(3, 0)^-$ series seen for $\mathrm{Ps^-}$ in figure 6 is missing for $\mathrm{H^-}$ in the same figure. Both in figure 5 and in figure 6 there are energy regions between prominent resonances where $\sigma(\hbar\omega; n = 2) > \sigma(\hbar\omega; n = 1)$ for $\mathrm{Ps^-}$ and $\sigma(\hbar\omega; n = 2) < \sigma(\hbar\omega; n = 1)$ for $\mathrm{H^-}$.

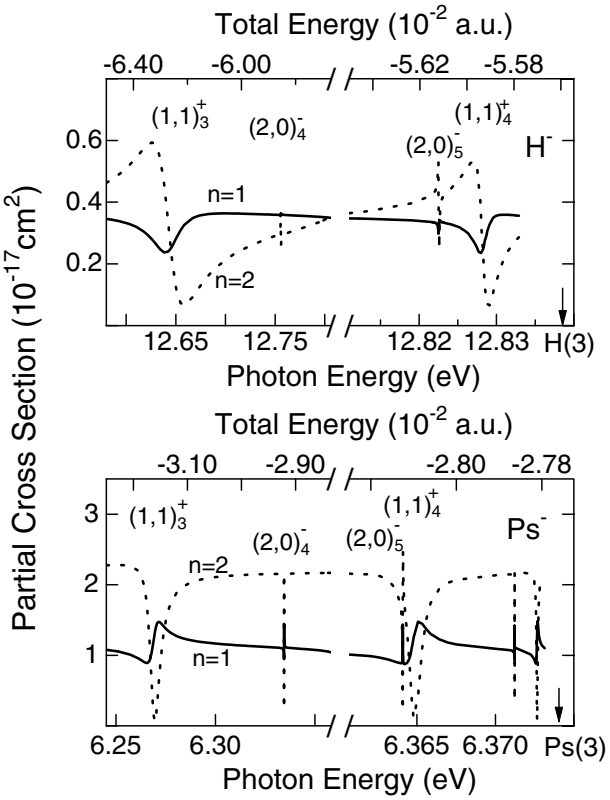

Figure 5. Partial photodetachment cross sections for the H^- and Ps^- systems below the $n = 3$ threshold indicated by vertical arrows. Full curve, $n = 1$ production; and dotted curve, $n = 2$ production.

The calculated resonance energies and widths are compared with the results of the complex-coordinate rotation method [9]–[11] in table 2. We include the resonance parameters calculated in terms of three basis sets: (a) all channel functions leading to Ps($n = 1$–4) + e$^-$, (b) all channel functions leading to Ps($n = 1$–3) + e$^-$, and (c) all channel functions leading to Ps($n = 1$–2) + e$^-$. The convergence behaviour of the resonance parameters near the Ps($n = 2$) threshold may give a rough estimate of the reliability of the present calculation. The resonance positions calculated with the basis sets (b) and (c) agree within three to four digits. Those with the basis sets (a) and (b) agree within four to five digits. The widths from these three basis sets agree within about 15%. Near the Ps($n = 2$) threshold, the channels detaching into e$^-$ + Ps($n = 2$) are weakly open or weakly closed and those detaching into e$^-$ + Ps($n = 3$) or e$^-$ + Ps($n = 4$) are strongly closed. We believe that the position of an $n'(K,T)^A_{n''}$ resonance calculated with all channels e$^-$ + Ps($n = 1$–n_c) is reliable to within about four digits if $n_c > n'$ and to within three digits if $n_c = n$, and that the width is reliable to within about 20% if $n_c \geq n$.

The agreement between the present resonance parameters and those by the complex-rotation method is good for resonances below the Ps($n = 3$) threshold. For resonances just below the Ps($n = 4$) threshold, the present and complex-rotation resonance positions agree to within about three digits. The widths of the $4(3,0)^-_6$, $4(2,1)^+_6$, and $4(3,0)^-_7$ resonances, however, disagree between the present work and the complex-rotation calculation.

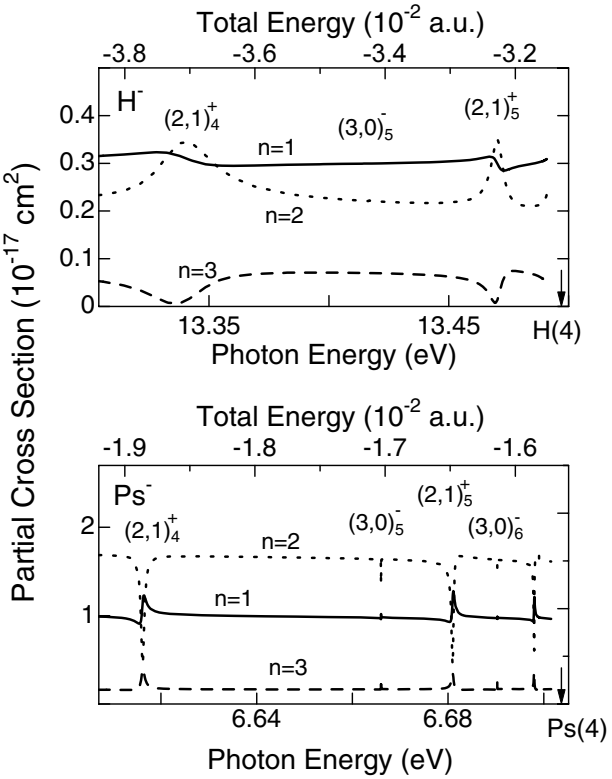

Figure 6. Partial photodetachment cross sections for the H^- and Ps^- systems below the $n = 4$ threshold indicated by vertical arrows. Full curve, $n = 1$ production; dotted curve, $n = 2$ production; and dashed curve, $n = 3$ production.

4. Summary

The HSCC method is used to calculate the total and partial photodetachment cross sections for the Ps^- system. The present total cross section agrees well with the variational calculations of Ward *et al* [5] below the photon energy of the cross section maximum, but is considerably lower than the result of [5] at higher energies. The off-resonance cross section below the Ps($n = 2$) threshold calculated by Igarashi *et al* [13] using a close-coupling method with a B-spline basis set agrees well with the present results at all the energies reported in [13]. A drastic increase in the present cross section occurs near the Ps($n = 2$) threshold due to Feshbach and shape resonances. Fine structures in the total and partial cross sections due to Feshbach resonances are found also just below the Ps($n = 3$) threshold and just below the Ps($n = 4$) threshold. The resonance parameters obtained in the present calculations are generally in good agreement with the results of the complex-coordinate rotation calculation [9]–[11].

The photodetachment cross sections of H^- and Ps^- are compared in detail both in the resonance regions and off resonance. They appear qualitatively similar to each other, although the detailed shapes of the corresponding resonances in H^- and Ps^- start to differ beyond the lowest Feshbach resonance below the $n = 3$ threshold. Some narrow resonances found in Ps^- below the Ps($n = 4$) threshold are without their counterparts in the H^- spectrum. The relative magnitudes of the partial cross sections at the higher photon energies depend strongly on the system.

Table 2. $^1\mathrm{P^o}$ resonances of the Ps^- system. E_r denotes the resonance energy in atomic units, Γ denotes the resonance width in atomic units, and $x[y] = x \times 10^y$.

Label $n(K,T)^A_{n'}$	Present (E_r, Γ)	Complex rotation (E_r, Γ)
$2(1,0)^-_3$	$(-6.3155[-2], 9.2[-7])^{a}$	$(-6.3156[-2], 1.0 \pm 0.3[-6])^{b}$
	$(-6.3156[-2], 9.8[-7])^{c}$	
	$(-6.3144[-2], 8.9[-7])^{d}$	
$2(1,0)^-_4$	$(-6.2543[-2], 2.5[-7])^{a}$	
	$(-6.2543[-2], 2.7[-7])^{c}$	
	$(-6.2542[-2], 2.4[-7])^{d}$	
$2(0,1)^+_2$	$(-6.2158[-2], 6.4[-4])^{a}$	$(-6.217[-2],\ \ 4.5 \pm 0.3[-4])^{e}$
	$(-6.2153[-2], 5.1[-4])^{c}$	
	$(-6.2174[-2], 5.4[-4])^{d}$	
$3(1,1)^+_3$	$(-3.1621[-2], 2.2[-4])^{a}$	$(-3.1622[-2], 2.2[-4] \pm 1[-7])^{b}$
	$(-3.1572[-2], 2.2[-4])^{c}$	
$3(2,0)^-_4$	$(-2.9212[-2], 1.5[-6])^{a}$	$(-2.9215[-2], 1.5 \pm 0.1[-6])^{b}$
	$(-2.9205[-2], 1.8[-4])^{c}$	
$3(2,0)^-_5$	$(-2.8125[-2], 6.0[-7])^{a}$	
	$(-2.8114[-2], 3.7[-7])^{c}$	
$3(1,1)^+_4$	$(-2.8099[-2], 3.3[-5])^{a}$	
	$(-2.8057[-2], 2.9[-5])^{c}$	
$3(2,0)^-_6$	$(-2.7864[-2], 8.7[-8])^{a}$	
	$(-2.7860[-2], 1.0[-7])^{c}$	
$3(1,1)^+_5$	$(-2.7811[-2], 3.5[-6])^{a}$	
	$(-2.7860[-2], 3.0[-6])^{c}$	
$4(2,1)^+_4$	$(-1.8863[-2], 3.2[-5])^{a}$	$(-1.8890[-2], 3.1 \pm 0.1[-5])^{f}$
$4(3,0)^-_5$	$(-1.7031[-2], 1.1[-6])^{a}$	$(-1.7041[-2], 1.3[-6])^{f}$
$4(2,1)^+_5$	$(-1.6480[-2], 2.0[-5])^{a}$	$(-1.6540[-2], 2.0 \pm 0.1[-5])^{f}$
$4(3,0)^-_6$	$(-1.6139[-2], 4.2[-7])^{a}$	$(-1.6161[-2], 4.7 \pm 5\ [-6])^{f}$
$4(2,1)^+_6$	$(-1.5855[-2], 6.4[-6])^{a}$	$(-1.5880[-2], 1.7 \pm 0.5[-5])^{f}$
$4(3,0)^-_7$	$(-1.5819[-2], 1.3[-7])^{a}$	$(-1.5803[-2], 2.5 \pm 2\ [-6])^{f}$

[a] Including all channels detaching into $\mathrm{e}^- + \mathrm{Ps}(n = 1\text{–}4)$.
[b] [9].
[c] Including all channels detaching into $\mathrm{e}^- + \mathrm{Ps}(n = 1\text{–}3)$.
[d] Including all channels detaching into $\mathrm{e}^- + \mathrm{Ps}(n = 1\text{–}2)$.
[e] [11].
[f] [10].

In the present work, all the channels detaching into $\mathrm{e}^- + \mathrm{Ps}(n = 1\text{–}4)$ have been coupled in solving the scattering equation of the $^1\mathrm{P^o}$ symmetry. Higher closed channels may need to be coupled to obtain more accurate resonance parameters and photodetachment cross sections close to the $n = 4$ threshold.

Appendix

Here we assess the convergence behaviour of the photodetachment cross section $\sigma(\hbar\omega; n)$ for the production of Ps(n), with respect to the number of channels included in the HSCC equations for the final continuum state. For this purpose we compare the cross section $\sigma^{(1-3)}(\hbar\omega; n)$ calculated including all channels detaching into $e^- + \mathrm{Ps}(n = 1\text{–}3)$ with the cross section $\sigma^{(1-4)}(\hbar\omega; n)$ calculated including all channels $e^- + \mathrm{Ps}(n = 1\text{–}4)$. The cross sections $\sigma^{(1-3)}(\hbar\omega; n)$ and $\sigma^{(1-4)}(\hbar\omega; n)$ agree with each other to within 1% for both $n = 1$ and $n = 2$ at total energies E below -0.03. Near the threshold $E_{\mathrm{Ps}(n=3)} = -0.027\,778$ for $e^- + \mathrm{Ps}(n = 3)$, however, some disagreement between the $n = 2$ cross sections starts to occur; at $E = -0.029$, for example, $\sigma^{(1-3)}(\hbar\omega; n = 2)$ is about 6% smaller than $\sigma^{(1-4)}(\hbar\omega; n = 2)$, although $\sigma^{(1-3)}(\hbar\omega; n = 1)$ and $\sigma^{(1-4)}(\hbar\omega; n = 1)$ agree with each other to within 0.2%. As E approaches the threshold $E_{\mathrm{Ps}(n=3)}$ further, the convergence in the cross section becomes slower and slower, although the gauge insensitivity is still well maintained. Thus, at $E = -0.027\,804$, $\sigma^{(1-3)}(\hbar\omega; n = 1)$ is about 15% larger than $\sigma^{(1-4)}(\hbar\omega; n = 1)$, and $\sigma^{(1-3)}(\hbar\omega; n = 2)$ is about 25% larger than $\sigma^{(1-4)}(\hbar\omega; n = 2)$. By generalizing this, we may infer, empirically, that the retention of all the channels in the HSCC equations up to and including the lowest-lying closed channels yields accurate cross sections $\sigma(\hbar\omega; n)$ except, possibly, very close to the threshold for the opening of another set of channels. This empirical rule was also found in previous applications of the HSCC method to the photoionization of He and photodetachment of H^- [18]. In the present production run, we include all channels up to $e^- + \mathrm{Ps}(n = 4)$. Therefore, the calculated cross sections are expected to be very accurate except very close to the threshold $E_{\mathrm{Ps}(n=4)} = -0.015\,625$ for Ps($n = 4$).

References

[1] See, for example, Ho Y K 1993 *Phys. Rev.* A **48** 4780
Frolov A M 1999 *Phys. Rev.* A **60** 2834
Korobov V I 2000 *Phys. Rev.* A **61** 064 503 and references therein
[2] Mills A P Jr 1981 *Phys. Rev. Lett.* **46** 717
[3] Mills A P Jr 1983 *Phys. Rev. Lett.* **50** 671
[4] Zafar N, Laricchia G, Charlton M and Garner A 1996 *Phys. Rev. Lett.* **76** 1595
Garner A J, Laricchia G and Özen A 1996 *J. Phys. B: At. Mol. Opt. Phys.* **29** 5961
[5] Ward S J, Humberston J W and McDowell M R C 1987 *J. Phys. B: At. Mol. Phys.* **20** 127
[6] Bhatia A K and Drachman R J 1985 *Phys. Rev.* A **32** 3745
[7] Ermolaev A M and Mandal C R 1988 *J. Phys. B: At. Mol. Opt. Phys.* **21** 2077
[8] Botero J and Greene C H 1986 *Phys. Rev. Lett.* **56** 1366
[9] Bhatia A K and Ho Y K 1990 *Phys. Rev.* A **42** 1119
[10] Ho Y K and Bhatia A K 1991 *Phys. Rev.* A **44** 2890
[11] Ho Y K and Bhatia A K 1993 *Phys. Rev.* A **47** 1497
[12] Ivanov I and Ho Y K 1999 *Phys. Rev.* A **60** 1015
[13] Igarashi A, Nakazaki S and Ohsaki A 2000 *Phys. Rev.* A **61** 032 710
[14] Macek J H 1968 *J. Phys. B: At. Mol. Phys.* **1** 831
[15] Fano U 1983 *Rep. Prog. Phys.* **46** 97
[16] Lin C D 1995 *Phys. Rep.* **257** 1
[17] Starace A F 1993 *Many-Body Theory of Atomic Structure and Photoionization*, ed T N Chang (Singapore: World Scientific) ch 5

[18] Tang J-Z and Shimamura I 1994 *Phys. Rev.* A **50** 1321
Tang J-Z and Shimamura I 1995 *Phys. Rev.* A **51** R1738
Tang J-Z and Shimamura I 1995 *Phys. Rev.* A **52** R3413
[19] Igarashi A, Shimamura I and Toshima N 1998 *Phys. Rev.* A **58** 1166
[20] Zhou Y and Lin C D 1995 *Phys. Rev. Lett.* **75** 2296
[21] Igarashi A, Toshima N and Shirai T 1994 *Phys. Rev.* A **50** 4951
[22] Gailitis M and Damburg R 1963 *Proc. Phys. Soc.* **82** 192
[23] Ohmura T and Ohmura H 1960 *Phys. Rev.* **118** 154
[24] Cortés M and Martín F 1993 *Phys. Rev.* A **48** 1227
[25] Lindroth E 1995 *Phys. Rev.* A **52** 2737
[26] Fano U and Cooper J W 1968 *Rev. Mod. Phys.* **40** 441
[27] Lin C D 1986 *Adv. At. Mol. Phys.* **22** 77
[28] Rost J-M 1994 *Hyperfine Interact.* **89** 343